

1 **Seismic noise recorded by telecommunication fiber optics reveal the impact of COVID-19**  
2 **measures on human activities**

3

4 Junzhu Shen<sup>1</sup> and Tieyuan Zhu<sup>1</sup>,

5 <sup>1</sup>Department of Geosciences, The Pennsylvania State University.

6 *Corresponding author:* Tieyuan Zhu ([tyzhu@psu.edu](mailto:tyzhu@psu.edu))

7

8 *Conflict of interest statement:* The authors declare no competing interests.

9 *Word count:* 3372

## 10 **Abstract**

11           Quantifying the response of human activities to different COVID-19 measures may serve  
12 as a potential way to evaluate the effectiveness of the measures and optimize measures. Recent  
13 studies reported that seismic noise reduction caused by less human activities due to COVID-19  
14 lockdown had been observed by seismometers. However, it is difficult for current seismic  
15 infrastructure in urban cities to characterize spatiotemporal seismic noise during the post-  
16 COVID-19 lockdown because of sparse distribution. Here we show key connections between  
17 progressive COVID-19 measures and spatiotemporal seismic noise changes recorded by a  
18 distributed acoustic sensing (DAS) array deployed in State College, PA. We first show  
19 spatiotemporal seismic noise reduction (up to 90%) corresponding to the reduced human  
20 activities in different city blocks during the period of stay-at-home. We also show partial noise  
21 recovery corresponding to increased road traffics and machines in Phase Yellow/Green. It is  
22 interesting to note that non-recovery seismic noise in 0.01-10 Hz suggests the low level of  
23 pedestrian movement in Phase Yellow/Green. Despite of a linear correlation between mobility  
24 change and seismic noise change, we emphasize that DAS recordings using city-wide fiber  
25 optics could provide a way for quantifying the impact of COVID-19 measures on human  
26 activities in city blocks.

27

## 28 **Introduction**

29           The COVID-19 pandemic has been impacting all aspects of our society, particularly  
30 public health and the economy. To reduce the spread of coronavirus, the COVID-19 measures  
31 such as working from home, self-isolation, and social distancing were implemented and resulted  
32 in a significant disruption to human activities. In the initial stage of the pandemic, the lockdown

33 measures were adopted, resulting in fewer human activities; after the lifting of containment  
34 measures, community life and economy restarted, leading to the recovery of human activities.  
35 Quantifying the response of human activities to different COVID-19 measures may serve as a  
36 potential way to evaluate the effectiveness of the measures and optimize measures in the future  
37 (Gupta et al., 2020; Jarvis et al., 2020).

38         Seismologically, human activities generate vibration noise with the frequency above 1 Hz  
39 (anthropogenic noise) (Bonney-Claudet et al., 2006). Several recent studies showed that a  
40 significant drop in high-frequency seismic noise levels (1–20 Hz) corresponded to fewer human  
41 activities after COVID-19 lockdown in the cities (Xiao et al., 2020; Poli et al., 2020; Lecocq et  
42 al., 2020; Yabe et al., 2020). These studies used a limited number of seismic stations in the cities  
43 to analyze the reduction of seismic noise attributed to the lockdown. Surprisingly, the recorded  
44 seismic data didn't show much distinguishable difference when the level of human activity  
45 changed during early isolation before official restrictions were placed and the period after the  
46 relaxation of restrictions (Dias et al., 2020; Pulli and Kafka, 2020). One possible reason is that  
47 seismic stations have difficulty picking up high-frequency anthropic noise afar due to the city's  
48 large spatial extent. During the COVID-19 pandemic, different sectors of the city might respond  
49 to the restrictions differently. This highly spatial-varying characteristic of anthropic noise brings  
50 the demand for dense seismic arrays in urban areas to provide high-resolution maps of noise  
51 variation.

52         Distributed acoustic sensing (DAS), a recent technology converting optic fibers to dense  
53 seismic sensor arrays, could provide high fidelity seismic strain/strain rate measurements at  
54 meter-scale spacing (Lindsey et al., 2017; Ajo-Franklin et al., 2019; Zhan et al., 2020; Lindsey  
55 and Martin, 2021). DAS has been used for seismic monitoring with tens of kilometers long

56 telecommunication fiber cables (Martin et al., 2018; Lindsey et al., 2019). Recent studies  
57 reported new recordings of vehicles, footsteps, and music, highlighting the sensitivity of DAS-  
58 equipped fibers in the cities (e.g., Wang et al., 2020; Zhu et al., 2021). Lindsey et al. (2020)  
59 reported using DAS with telecommunication fiber to discriminate the traffic noise reduction in  
60 different areas (grocery store and hospital) during the COVID-19 pandemic.

61       Using an underground telecommunication fiber-optics DAS array in State College, PA,  
62 USA (Figure 1a), we show significant seismic noise variation from March to June 2020  
63 responding to progressive COVID-19 measures: stay-at-home, Phase Yellow, and Phase Green.

64

#### 65 **The DAS array**

66       The continuous data we use were collected by the Penn State FORESEE (Fiber-Optics  
67 For Environment Sensing) array of underground telecommunication fiber optic cables. The DAS  
68 array had a total of 2137 sensors with a 10 m gauge length and 2 m channel spacing. The  
69 continuous strain rate measurements are sampled at 500 Hz. We downsampled the data to 250  
70 Hz considering the efficiency in terms of computation and storage. Owing to the unexpected  
71 power disruptions, there are no recordings between March 16 – April 15 and May 06 – 26. We  
72 analyzed seismic noise variation of 21 weekdays at seven distinct time periods (3 days for each  
73 group) from March 3 – June 10, 2020, covering the normal spring semester, spring break,  
74 quarantine after the stay-at-home order was issued and the gradual relaxation of the COVID-19  
75 measures.

76       Our DAS array, which is located at the biggest institution in the town, Penn State  
77 University, offers opportunities to explore the social response at city-block scales to  
78 Pennsylvania’s progressive lockdown measures that rely on voluntary community action. Penn

79 State University was closed after spring break on March 18, 2020, and all the residents were  
80 required to stay at home, except for essential movements according to the statewide stay-at-home  
81 order from April 1, 2020. The social activities started to recover after the official relaxation  
82 (designated Phase Yellow/Green) on May 27, 2020.

83

#### 84 **Spatial distribution of noise variation during COVID-19**

85 We first present the meter-scale spatial variation of seismic noise (RMS strain rate,  
86 calculation details in Text S1) across the 5-km DAS array (Figure 1b). Spatially, during the  
87 entire period, the seismic RMS noise data were impacted mostly on the main campus, exhibiting  
88 the slightest variation in agricultural/sports fields (AG area) and the intermediate variation in the  
89 western campus. A significant drop of seismic RMS noise was observed after the implementation  
90 of the stay-at-home measure. After Phase Yellow, seismic noise recovered somewhat but was  
91 maintained at a relatively low level.

92 To understand the spatial variation of seismic noise at a 2-meters spacing over the entire  
93 array, we calculated the RMS strain rate over 10 hours from 8 am to 6 pm. We repeated the  
94 calculation for data on March 5 (spring semester), April 16 (during the stay-at-home order) and  
95 June 4 (business reopening) (all Thursdays) and compared with the average daytime RMS strain  
96 rate during a week of the spring semester (February 3–7 2020).

97 Figure 2 shows the seismic noise spatial variation on March 5 (before the pandemic),  
98 April 16 (stay-at-home), and June 4 (Phase Green). By analyzing noise in four frequency bands  
99 (0.01–1 Hz, 1–10 Hz, 10–50 Hz, and 50–100 Hz), we could distinguish which frequency band of  
100 noise was affected by the COVID-19 measures most.

101 First, the biggest noise variation is detected on the main campus (Figure 2b). The peak  
102 noise reduction appears in all frequency bands on April 16 under the stay-at-home order. The  
103 largest reduction in the main campus could be up to 90% in the frequency band 1–10 Hz. With  
104 the gradual relaxation of the COVID-19 measure policies, the noise level on the main campus  
105 increases but remains relatively low (about 60% in 1–10 Hz). Exceptions can be found around  
106 Ch 1535–1580, where the noise level is higher during the stay-at-home order, possibly because  
107 cars were allowed to enter this area and generated stronger noise than previous pedestrian-only  
108 period (restricted before the school closure).

109 Both AG area and western campus area exhibited less university-related activity. Hence,  
110 the noise variation is relatively stable in all frequency bands. The largest noise reduction is in  
111 10–50 Hz, which was likely caused by the decrease in traffic (e.g., school buses and commuter  
112 vehicles) due to the COVID-19 lockdown measures. On the western campus, significant noise  
113 variation near the end of the array is likely caused by the transition between shutdown (stay-at-  
114 home order) and opening (regular semester/Phase Green) of construction-related activities.

115 We also found that channels around the intersections could detect large noise variation in  
116 the frequency band below 50 Hz while noise levels of adjacent channels away from the road  
117 remained unchanged. Our fiber array could identify the exact places where traffic noise is  
118 dominant, which could help estimate the number of vehicles (Lindsey et al., 2020).

119

## 120 **Identification of noise sources associated with human activities**

121 Predominant anthropogenic noise sources vary in different city sectors, among  
122 workplaces (Ch 1240–1440), main roads (Ch 850–1110), a residential area (Ch 690–830) and a  
123 less populated area (Ch 110–300) (Figure 1b and 2). Characterizing seismic noise from particular

124 sources can help us understand local social interactions with city lockdown measures. Our 5-km-  
125 long dense DAS array at 2 m spacing covers plenty of public infrastructures. Hence, we chose  
126 specific subarrays and identified noise sources – footstep signals, passing vehicles and industrial  
127 noise, by comparing seismic noise variations before and after the COVID-19 restrictions.

128         To analyze the impact of lockdown measures on footsteps, we selected 1-hour data (local  
129 time 10 am–11 am) from a subarray beneath a pedestrian-only path on the main campus for  
130 similar days (March 5, April 16, and June 4) (Figure 3). Intuitively, walking footstep signals  
131 showed up in the data as linear streaks with a slow moveout (1–2 m/s). On March 5, during the  
132 regular semester, the DAS array picked up many walking signals (plenty of data streaks in Figure  
133 3a). Contrarily on April 16, after the stay-at-home order was issued, only a few signals are  
134 detected on this path (Figure 3b). In Phase Green (June 4), the footstep signals are almost not  
135 recovered despite the easing of some restriction measures. This invariability is confirmed by the  
136 average spectrum plot in Figure 3d, showing the absence of peaks at 2 Hz and 4 Hz in both April  
137 16 and June 4 curves, which are considered as the footstep signals (Zhu et al., 2021).

138         We next analyzed traffic noise recordings (Figures 3e-h) from a subarray beneath Curtin  
139 Road, the main road on campus. There is a significant decrease in passing vehicles when  
140 comparing data between March 5 and April 16. This is due to the shutdown of the university  
141 preventing people from traveling to campus. The bus service was also reduced. On June 4, more  
142 linear signals indicate more passing vehicles. The decrease-increase traffic noise pattern is  
143 obviously different from the loss-to-flat pattern of pedestrian movement. This trend is also  
144 confirmed in the frequency spectrum (Figure 3h): a significant drop of the power spectra  
145 between 10 and 50 Hz about 20 dB, then an increase by 5 dB. We interpreted 10–50 Hz as the  
146 frequency band of passing vehicles.

147 In addition, we identified higher frequency noise associated with construction activities.  
148 On the western campus, a new parking garage and utility upgrades near the fibers were planned  
149 to be constructed from December 17, 2019, to April 20, 2021. Due to the suspension of the  
150 industrial activity during the stay-at-home measures, the data on April 15 show no detected  
151 events (Figure 3i). After restarting industrial activities since May 7 (Phase Yellow), we observe  
152 strong industrial noise on June 1 in Figure 3j. The noise in the frequency band of 10–30 Hz could  
153 be identified as noise from construction vehicles and the broadband impulses (10–100 Hz)  
154 between 11:09 – 11:10 am were from machinery, which produced short bursts of vibrations.

155

#### 156 **Temporal noise variation during COVID-19**

157 While significant noise variations across the array are detected, here we show the  
158 complete temporal noise variations from March 3 to June 10, 2020. Figure 4 shows the time-  
159 lapse noise changes recorded by Ch 981 located beneath Curtin Road on the main campus (Ch  
160 204 in Figure S1 and Ch 1491 in Figure S2). As a comparison, seismic noise changes are plotted  
161 against the Google mobility data from workplaces and transport across the county (details in  
162 Text S2). Although detailed mobility data near the fiber are unavailable, a general validation  
163 could be conducted.

164 First, we can see that noise experienced a slight decrease (up to 10%) in the spring break  
165 compared to the regular spring semester in the low-frequency band (0.01–10 Hz). This decrease  
166 (<10 Hz) is attributed to the least school activities during spring break (i.e., many students left  
167 school and there were few school activities). In 10–50 Hz, the noise changes in both Ch 981  
168 (Figure 4) and Ch 1491 (Figure S2c) remain flat before the stay-at-home order, while the change  
169 in Ch 204 (Figure S1) decreases. During spring break, the quiet roads (Ch 204) are more likely to

170 have reduced vehicle traffic while the main road on campus (Ch 981 and 1491) might remain  
171 busy (e.g., citizens driving across the campus and regular bus services). In the high-frequency  
172 range (50–100 Hz), the noise changes only decrease in channel 1491 (Figure S2d), which is  
173 likely caused by stopping machinery noise (from a construction site near Ch 1491).

174         After the university closure on March 18, a distinct drop (up to 60% daily average) of  
175 noise levels falls to the lowest level in the whole period of the stay-at-home phase (Figures 2 and  
176 S1 and S2). Moreover, this universal noise reduction in all frequency bands (0.01–100 Hz)  
177 reflects the quieter period and the huge reduction of noise sources due to the stay-at-home order.  
178 We inferred that the campus had very few human activities.

179         After Phase Yellow on May 27, the noise level (0.01–10 Hz) still stays flat at the lowest  
180 level (50%~60% reduction) until Phase Green. This feature implies that residents continued to  
181 follow the stay-at-home guidelines (e.g., working at home). Interestingly, the noise level (10–100  
182 Hz) increases gradually, which is consistent with the mobility data (transport), suggesting the  
183 recovery of road traffics and industrial activities (e.g., shopping and construction business). After  
184 Phase Green, the noise in all frequency bands gradually increases by a few percentages (1–10  
185 Hz) to 20% (0.01-1 Hz).

186         We calculated the root mean square error (RMSE) between Google mobility data from  
187 two categories and noise changes in four frequency bands discussed above (Figure 4). A smaller  
188 RMSE represents a better correlation with the mobility data in a particular category. We interpret  
189 noise sources in the frequency bands of 0.01–1, 1–10, 10–50, 50–100 Hz as school activities  
190 mixed with bedrock loading of vehicles (Lindsey et al., 2020); school activities; traffic signals;  
191 traffic signals mixed with industrial activities, respectively.

192

## 193 **Comparison to mobility data**

194 To generalize the relationship between seismic noise and mobility data, we calculated an  
195 averaged seismic noise change for a single day by first averaging 24 hours noise changes for  
196 each channel and then averaging them across all channels. Figure 5 shows a crossplot between  
197 the noise data and Google mobility data. The noise reduction in the frequency band of 1–10 Hz is  
198 compared with the workplace mobility data, while the 10–50 Hz noise level reduction is  
199 compared with transport mobility data. The good linear correlation between mobility change and  
200 changes of seismic noise level allows us to relate variation of seismic noise level and mobility  
201 changes as,

$$202 \quad M_{TL} = 1.49 N_{TL}$$

203 where  $M_{TL}$  is time-lapse mobility change and  $N_{TL}$  is time-lapse noise change. This linearity  
204 implies that the seismic noise variation (1–50 Hz) is linearly proportional to the amount of  
205 human activities, including foot traffic and road traffic.

206

## 207 **Discussion and Conclusions**

208 While a general noise reduction was discovered in many cities by previous studies (Xiao  
209 et al., 2020; Poli et al., 2020; Lecocq et al., 2020; Dias et al., 2020; Yabe et al., 2020), our results  
210 reveal many new and detailed features of seismic noise caused by progressive COVID-19  
211 measures.

212 First, we find the seismic noise reduction in broad frequency bands (0.01–100 Hz) caused  
213 by decreased human activities during the period of stay-at-home (March-April 2020). After  
214 Phase Yellow (May-June 2020), the seismic noise recovers slightly in high-frequency bands (10–  
215 100 Hz), while the noise in 1–10 Hz shows no recovery until late Phase Green. We interpret that

216 after the relaxation of restrictions, residents voluntarily followed the stay-at-home guidelines  
217 (i.e., less pedestrian movement) while road traffic and industrial activities started to recover.  
218 These results show that the dense DAS array in urban areas could sense slight changes due to the  
219 gradual lifting of restrictions since the end of May. Noise changes caused by particular human  
220 activities (e.g. pedestrian movements and industrial activities) can also be identified in different  
221 frequency bands. The sensitivity of the DAS array indicates the possibility of using seismic noise  
222 variation from telecom DAS in the city-block scale to evaluate local response to social  
223 restrictions.

224         Second, seismic noise in the low frequency band (0.01–1 Hz, where anthropogenic noise  
225 is weaker) is also impacted by the COVID-19 measures, which was not reported in previous  
226 studies using seismic networks (Xiao et al., 2020; Lecoq et al., 2020; Poli et al., 2020). Lindsey  
227 et al. (2020) observed a reduction in the very-low-frequency seismic noise (0.01–1 Hz) using  
228 fiber sensors along a major road in Stanford, CA, during the COVID-19 pandemic. This  
229 reduction is likely to be the geodetic response of the roadbed to decreased vehicle loading  
230 (Lindsey et al., 2020; Jousset et al., 2018), providing an additional constraint to quantify the  
231 number of passing vehicles using dense seismic noise data.

232         Third, the meter scale human activity variation is hard to be obtained from either sparse  
233 seismic stations or mobility data due to incomplete data acquisition, location accuracy, and  
234 privacy issues. In contrast, DAS could provide a high spatial resolution map of seismic noise  
235 variation, which can distinguish different human activity variation patterns between the main  
236 campus and agricultural area, and further identify dominant noise sources on different streets  
237 within each area. For instance, the significant noise reduction, almost 90% in the frequency band  
238 1-50 Hz, on the main campus is attributed to few local concentrated human activities (including

239 footsteps and road traffic) due to the required stay-at-home order in State College PA. Seismic  
240 noise in less busy areas (AG areas) remains relatively stable. In the local noise reduction zone  
241 (main campus), we could distinguish footsteps, single passing vehicles, and high-frequency  
242 industrial noise associated with construction activities (Figure 3). The spatial noise variation  
243 provides detailed information on population mobility dynamic in urban areas, demonstrating that  
244 the lockdown measurements have a significant impact on certain populated areas (e.g.,  
245 universities) during the COVID-19 pandemic.

246         Finally, a linear correlation between mobility change and seismic noise change implies  
247 that high-resolution DAS seismic noise data could further serve as an additional and innovative  
248 approach for evaluating the impact of the COVID-19 measures in populated areas related to  
249 industrial, educational, and other activities. DAS data contain non-personalized information and  
250 enable urban monitoring use patterns, which protects the privacy of individuals compared to cell  
251 phone location-tracking data (Lindsey and Martin, 2021). This suggests the benefits of using city  
252 infrastructure fiber-optic cables over the mobility data to monitor and quantify human activity in  
253 a city (e.g., estimation of people’s movement and the number of vehicles) with high  
254 spatiotemporal resolution.

255         In summary, our results show key connections between the progressive COVID-19  
256 measures and spatiotemporal seismic noise changes using a dense fiber array at the city scale,  
257 which helps estimate whether and how communities respond to county-level policies. Our  
258 research shows that seismic noise recorded by infrastructure DAS fiber networks could  
259 potentially help policymakers to evaluate the compliance of the population following state-  
260 mandated mobility restrictions, which in-turn could optimize the restriction policies in the future  
261 pandemic. Looking forward, fiber-optic arrays using existing telecommunication fiber networks

262 make seismic monitoring more cost-effective and practical than other types of seismic sensors in  
263 urban areas.

264

265

## 266 **Data and Resources**

267         The DAS data used in this study are collected by the Penn State FORESEE array of  
268 underground telecommunication fiber optic cables. Calculated seismic noise level and raw DAS  
269 data used for plotting figures in this paper are available for download at  
270 <https://doi.org/10.5281/zenodo.4072484>. The mobility data are released by Google at  
271 <https://www.google.com/covid19/mobility/> (last accessed: 25 September 2020). We used  
272 ArcGIS Pro to make Figure 1a. Supplemental Material for this article includes: 1) methods about  
273 the calculation of the RMS noise changes; 2) a description of Mobility Data we used; 3) two  
274 figures of temporal noise level changes at Ch 204 and 1491.

275

## 276 **Acknowledgments**

277         We thank Eileen Martin, Zi Xian Leong and Sam Hone for proofreading the article. We  
278 thank Chris Marone for his warm support to convince the Penn State Institute of Natural Gas  
279 Research to provide seed money to the DAS fiber array. We thank Todd Myers, Ken Miller at  
280 Penn State University, Thomas Coleman from Silixa Inc. who help setup the fiber-optic DAS  
281 array. The DAS array was supported by Penn State Institute of Environment and Energy seed  
282 grant and Institute of Natural Gas Research.

283

## 284 **References**

285 Ajo-Franklin, J. B., S. Dou, N. J. Lindsey, I. Monga, C. Tracy, M. Robertson, V. Rodriguez  
286 Tribaldos, C. Ulrich, B. Freifeld, T. Daley, et al. (2019). Distributed Acoustic Sensing Using  
287 Dark Fiber for Near-Surface Characterization and Broadband Seismic Event Detection, *Sci*  
288 *Rep* 9, no. 1

289 Bonnefoy-Claudet, S., F. Cotton, and P.-Y. Bard (2006). The nature of noise wavefield and its  
290 applications for site effects studies, *Earth-Science Reviews* 79, no. 3–4, 205–227

291 Dias, F. L., M. Assumpção, P. S. Peixoto, M. B. Bianchi, B. Collaço, and J. Calhau (2020).  
292 Using Seismic Noise Levels to Monitor Social Isolation: An Example From Rio de Janeiro,  
293 Brazil, *Geophys. Res. Lett.* 47, no. 16

294 Google (2020). COVID-19 Community Mobility Reports. Available at:  
295 <https://www.google.com/covid19/mobility/> (accessed: 25 September 2020).

296 Gupta, S., T. Nguyen, F. L. Rojas, S. Raman, B. Lee, A. Bento, K. Simon, and C. Wing (2020).  
297 Tracking Public and Private Responses to the COVID-19 Epidemic: Evidence from State and  
298 Local Government Actions, National Bureau of Economic Research

299 Jarvis, C. I., K. Van Zandvoort, A. Gimma, K. Prem, P. Klepac, G. J. Rubin, and W. J. Edmunds  
300 (2020). Quantifying the impact of physical distance measures on the transmission of COVID-  
301 19 in the UK, *BMC Med* 18, no. 1

302 Jousset, P., T. Reinsch, T. Ryberg, H. Blanck, A. Clarke, R. Aghayev, G. P. Hersir, J. Henningses,  
303 M. Weber, and C. M. Krawczyk (2018). Dynamic strain determination using fibre-optic  
304 cables allows imaging of seismological and structural features, *Nat Commun* 9, no. 1

305 Lecocq, T., S. P. Hicks, K. Van Noten, K. van Wijk, P. Koelemeijer, R. S. M. De Plaen, F.  
306 Massin, G. Hillers, R. E. Anthony, M.-T. Apoloner, et al. (2020). Global quieting of high-

307 frequency seismic noise due to COVID-19 pandemic lockdown measures, *Science* 369, no.  
308 6509, 1338–1343

309 Lindsey, N. J., and E. R. Martin (2021). *Fiber-Optic Seismology*, *Annu. Rev. Earth Planet. Sci.*  
310 49, no. 1

311 Lindsey, N. J., E. R. Martin, D. S. Dreger, B. Freifeld, S. Cole, S. R. James, B. L. Biondi, and J.  
312 B. Ajo-Franklin (2017). *Fiber-Optic Network Observations of Earthquake Wavefields*,  
313 *Geophys. Res. Lett.* 44, no. 23, 11,792-11,799 Lindsey, N. J., T. C. Dawe, and J. B. Ajo-  
314 Franklin (2019). *Illuminating seafloor faults and ocean dynamics with dark fiber distributed*  
315 *acoustic sensing*, *Science* 366, no. 6469, 1103–1107

316 Lindsey, N. J., S. Yuan, A. Lellouch, L. Gualtieri, T. Lecocq, and B. Biondi (2020). *City-Scale*  
317 *Dark Fiber DAS Measurements of Infrastructure Use During the COVID-19 Pandemic*,  
318 *Geophys. Res. Lett.* 47, no. 16

319 Martin, E. R., F. Huot, Y. Ma, R. Cieplicki, S. Cole, M. Karrenbach, and B. L. Biondi (2018). *A*  
320 *Seismic Shift in Scalable Acquisition Demands New Processing: Fiber-Optic Seismic Signal*  
321 *Retrieval in Urban Areas with Unsupervised Learning for Coherent Noise Removal*, *IEEE*  
322 *Signal Process. Mag.* 35, no. 2, 31–40

323 McNamara, D. E. (2004). *Ambient Noise Levels in the Continental United States*, *Bulletin of the*  
324 *Seismological Society of America* 94, no. 4, 1517–1527

325 Poli, P., J. Boaga, I. Molinari, V. Cascone, and L. Boschi (2020). *The 2020 coronavirus*  
326 *lockdown and seismic monitoring of anthropic activities in Northern Italy*, *Sci Rep* 10, no. 1

327 Pulli, J., & Kafka, A. (2020) *Disentangling Anthropomorphic Noise Sources During the COVID-*  
328 *19 Virus Lockdowns: Examples from the Washington DC and Boston Areas*. *ES-SSA Annual*  
329 *Meeting 2020*

330 Wang, X., E. F. Williams, M. Karrenbach, M. G. Herráez, H. F. Martins, and Z. Zhan (2020).  
331 Rose Parade Seismology: Signatures of Floats and Bands on Optical Fiber, Seismological  
332 Research Letters 91, no. 4, 2395–2398

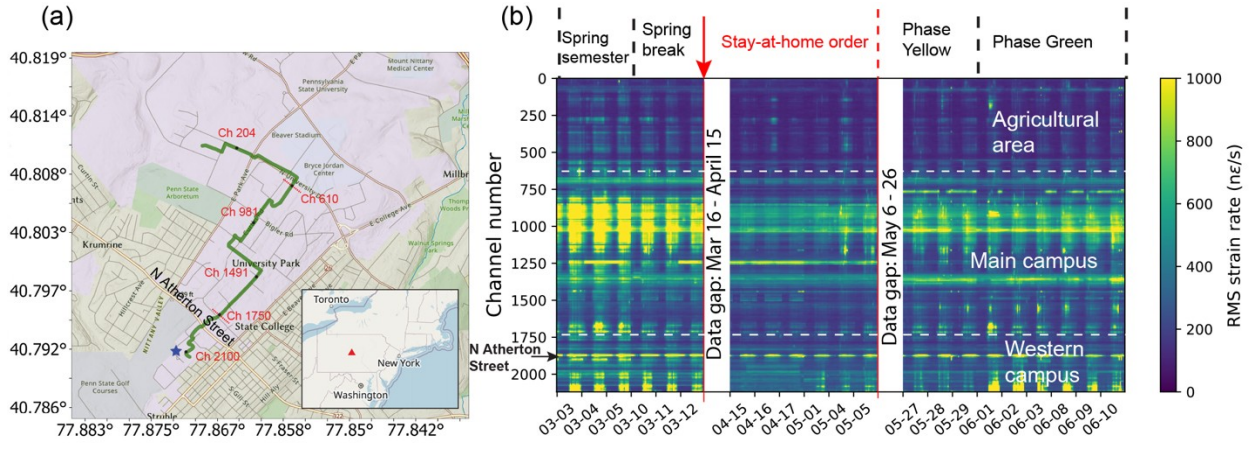
333 Xiao, H., Z. C. Eilon, C. Ji, and T. Tanimoto (2020). COVID-19 Societal Response Captured by  
334 Seismic Noise in China and Italy, Seismological Research Letters 91, no. 5, 2757–2768

335 Yabe, S., K. Imanishi, and K. Nishida (2020). Two-Step Seismic Noise Reduction Saused by  
336 COVID-19 Induced Reduction in Social Activity in Metropolitan Tokyo, Japan, Research  
337 Square

338 Zhan, Z. (2019). Distributed Acoustic Sensing Turns Fiber–Optic Cables into Sensitive Seismic  
339 Antennas, Seismological Research Letters 91, no. 1, 1–15

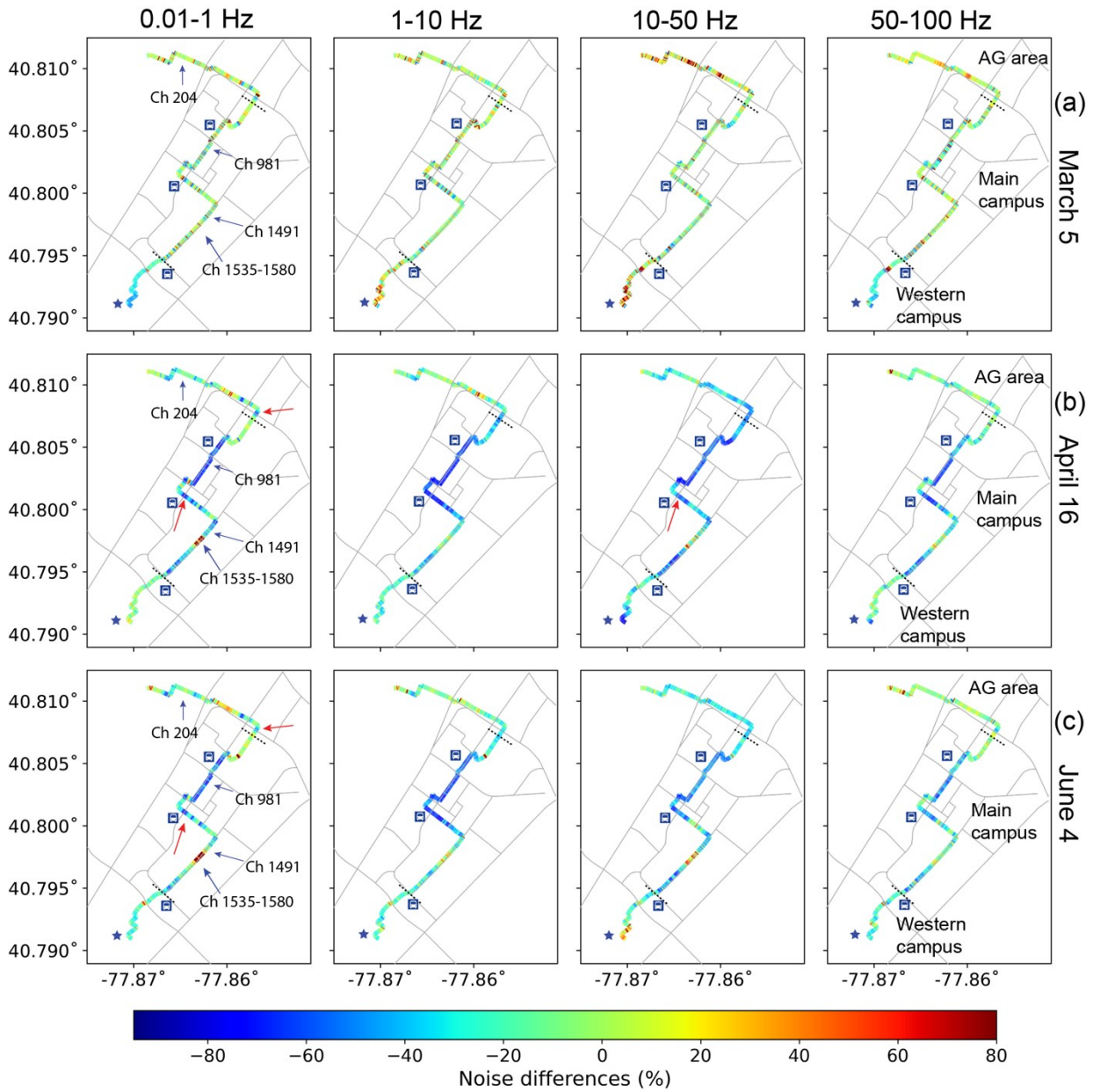
340 Zhu, T., J. Shen, and E. R. Martin (2021). Sensing Earth and environment dynamics by  
341 telecommunication fiber-optic sensors: an urban experiment in Pennsylvania, USA, Solid  
342 Earth 12, no. 1, 219–235

343 **Figures**



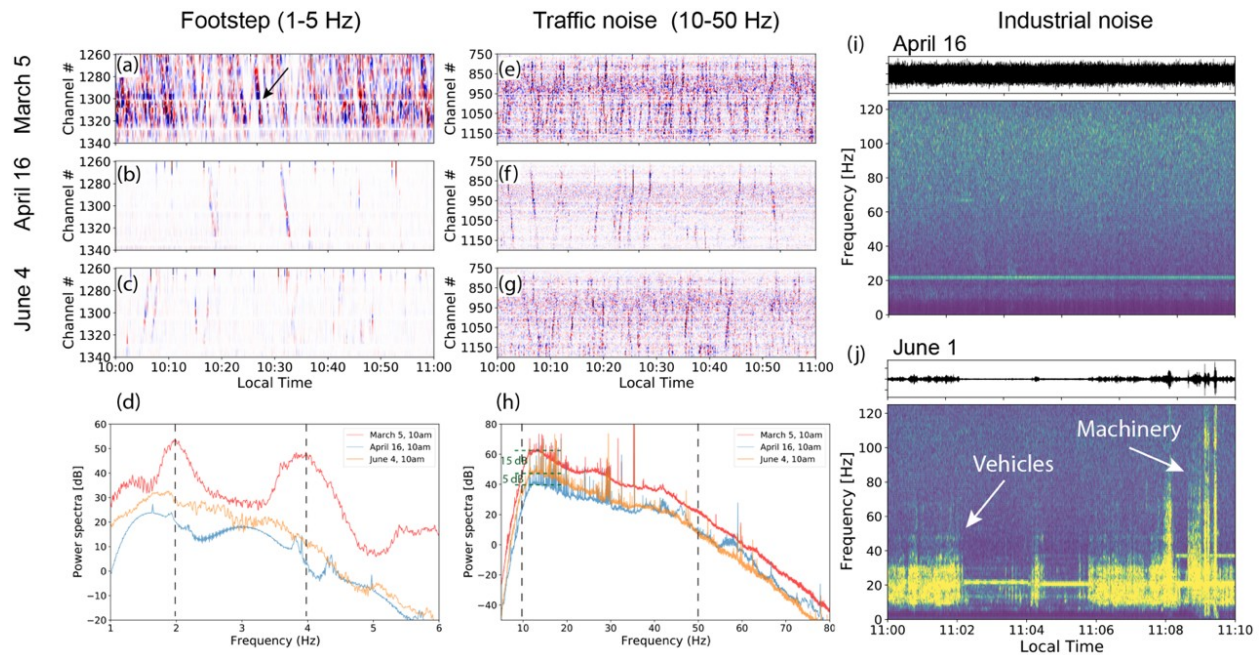
344

345 **Figure 1.** (a) DAS map. Dark fiber (Green line) is located beneath Penn State University campus  
346 in State College, Pennsylvania (inset, red triangle). Selected channels are indicated for  
347 referencing sensors' location. The blue star indicates the construction site. The red dashed lines  
348 divide the campus into three sections. (b) Temporal variations of seismic noise across the DAS  
349 channels. The timeline of local conditions is shown above. Note that dates are not continuous  
350 and the white space indicates the data gaps due to unexpected power interruptions. Red line  
351 marks the abrupt noise change during the implementation of the stay-at-home order. A Clear  
352 diurnal pattern shows that signals are mainly from human activities in the daytime.



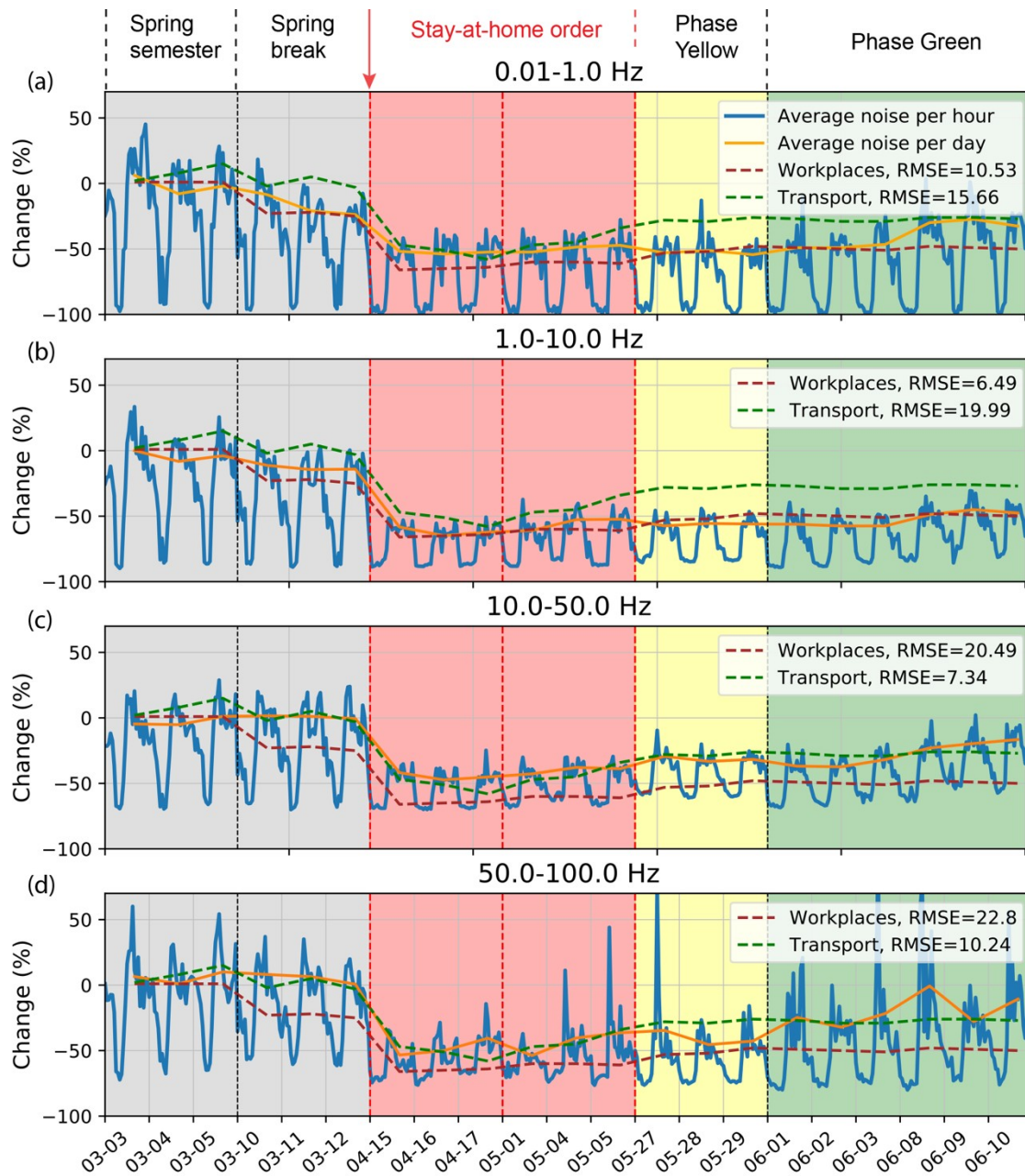
353

354 **Figure 2.** Time-lapse noise variations across the DAS array. The time-lapse noise difference is  
 355 calculated on a given day relative to baseline: March 5 before the pandemic in the regular school  
 356 semester (a), April 16 during stay-at-home order (b) and June 4 during Phase Green (c). Bus  
 357 stops and the construction site are shown on the map. Red arrows indicate the noise reduction at  
 358 intersections.



359

360 **Figure 3.** DAS recordings of footsteps on March 5, April 16, and June 4 (a-c) and traffic noise  
 361 (e-g). Corresponding power spectra (d and h) from the seismograms above (a-c and e-g) were  
 362 averaged over each subarray. Comparisons of construction-related seismic noise in the stay-at-  
 363 home order (April 16, 2020) and in Phase Green (June 1, 2020). We selected DAS recordings at  
 364 Ch 2100 next to the construction site (its location is indicated in Figure 1a). Raw DAS data and  
 365 their time-frequency spectra maps on (i) April 16, 2020 and (j) June 1, 2020. The 20-Hz signal  
 366 might be caused by the nearby air conditioner.

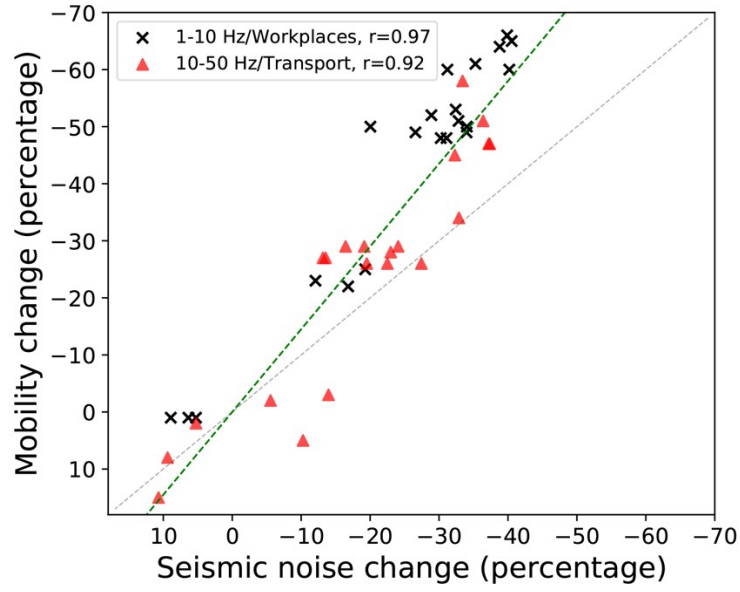


367

368 **Figure 4.** Noise change at Ch 981 in the frequency range of (a) 0.01-1 Hz, (b) 1-10 Hz, (c) 10-50

369 Hz and (d) 50-100 Hz. The daily average noise change (orange) and the mobility data from

370 Google (dashed line) are plotted.



371

372 **Figure 5.** Plot of average time-lapse changes in seismic noise (1-10 Hz and 10-50 Hz) from all  
 373 channels against with Google mobility data from workplaces and transport, respectively. Each  
 374 data point represents the averaged changes on a single day (the same days in Figure 1b and 4).  
 375 The green dashed line indicates the linear correlation between mobility change and seismic noise  
 376 change with a ratio of 1.49. The diagonal gray line indicates a ratio of 1.